NACA RM A51E15

NACA

RESEARCH MEMORANDUM

THE USE OF TWO-DIMENSIONAL SECTION DATA TO ESTIMATE THE LOW-SPEED WING LIFT COEFFICIENT AT WHICH SECTION STALL FIRST APPEARS ON A SWEPT WING

By Ralph L. Maki

Ames Aeronautical Laboratory
Moffett Field, Calif.

CLASSIFICATION CANCELLED

Authority J. W. Crowley Date 12-7-53

By T.C.F. Release form no. 1647

NATIONAL ADVISORY COMMITTEE
FOR AERONAUTICS

WASHINGTON

July 27, 1951

NATIONAL ADVISORY COMMITTEE FOR AERONAUTICS

RESEARCH MEMORANDUM

THE USE OF TWO-DIMENSIONAL SECTION DATA TO ESTIMATE THE LOW-SPEED WING LIFT COEFFICIENT AT WHICH SECTION STALL FIRST APPEARS ON A SWEPT WING

By Ralph L. Maki

SUMMARY

A procedure for estimating the wing lift coefficient for and the spanwise location of the first occurrence of section stall on a swept wing is presented. The procedure is based on an existing method applicable to unswept wings. This existing method is extended and modified as necessary to account for the effects of sweep. Simplified lifting-surface theory and two-dimensional section data are utilized, with due consideration given to the concepts of simple sweep theory. The procedure is applied to a swept-wing model with and without trailing-edge split flaps, and with several modifications made to the wing leading edge. Comparison of the various predicted and experimental values of wing lift coefficient for and spanwise location of the first occurrence of section maximum lift showed the following: The predictions of absolute wing lift coefficient were from 0.1 to 0.2 low in most cases; the predictions of the increments in wing lift coefficient attributable to the various leading-edge modifications were usually quite accurate; the predictions of the spanwise location could not be rigorously checked but appeared to be approximately correct. A brief application of the method to other wing plan forms gave results that were comparable to the results of the model described and tested in this report.

INTRODUCTION

It has been well established that for swept wings, as for straight wings, noticeable changes in some or all of the aerodynamic characteristics occur when the flow separates from some part of the wing. In the case of straight wings, this occurs at, or very near, wing maximum lift.

In the case of swept wings, however, the flow separation generally occurs well below wing maximum lift. The separation generally results in undesirable changes in aerodynamic characteristics of sufficient magnitude to restrict the usable lift to values below maximum lift. A method which relates the stalling of a swept wing to the maximum lift of its airfoil sections would be useful in devising means for improving the high lift characteristics of swept wings. References 1 and 2 present a method which utilizes airfoil section data to predict the first occurrence of section stall on straight wings. It is the purpose of this report to account for the effects of wing sweep so as to extend the applicability of the method to swept wings, and to evaluate the revised method with the aid of experimental results obtained from study of a particular model with several wing modifications.

NOTATION

The test data are presented as standard NACA coefficients of forces and moments. Moments on the swept-wing model are referred to a point 1 inch above the fuselage center line and to a fore-and-aft position corresponding to the quarter-chord point of the mean aerodynamic chord.

A aspect ratio $\left(\frac{b^2}{S}\right)$

b wing span, measured perpendicular to the plane of symmetry of the swept-wing model, feet

c wing chord, measured in the free-stream direction, feet

$\bar{c}$ mean aerodynamic chord, measured in the free-stream direction $\left(\frac{\int_0^{b/2} c^2 dy}{\int_0^{b/2} c\, dy}\right)$, feet

c_c chord-force coefficient $\left(\frac{\text{chord force}}{qc}\right)$

C_D drag coefficient of the swept-wing model $\left(\frac{\text{drag}}{qS}\right)$

C_{D_T} increment of drag coefficient of the swept-wing model due to wind-tunnel-wall interference

c_l section lift coefficient $\left(\frac{\text{section lift}}{qc}\right)$

c_{l_b} section lift coefficient due to basic loading on the wing at zero wing lift

c_{l_f} section lift coefficient due to flap deflection at constant angle of attack

c_{l_i} section lift coefficient due to camber measured at the ideal angle of attack of the section

C_L lift coefficient of the swept-wing model $\left(\frac{\text{lift}}{qS}\right)$

C_m pitching-moment coefficient of the swept-wing model $\left(\frac{\text{pitching moment}}{qS\bar{c}}\right)$

c_n normal-force coefficient $\left(\frac{\text{normal force}}{qc}\right)$

P local pressure coefficient $\left[\frac{(\text{local static pressure})-(\text{free-stream static pressure})}{q}\right]$

q free-stream dynamic pressure, pounds per square foot

R Reynolds number $\left(\frac{V\bar{c}}{\nu}\right)$

S wing area, square feet

V free-stream velocity, feet per second

x distance from original airfoil leading edge, measured parallel to chord line, feet

y spanwise distance from the wing center line, feet

α free-stream angle of attack of the swept-wing model, with reference to the wing-chord plane, degrees

α_o angle of attack of the two-dimensional model, degrees

α_T increment of angle of attack due to wind-tunnel-wall interference, degrees

δ_f flap deflection, measured perpendicular to the hinge line, degrees

η spanwise station $\left(\frac{2y}{b}\right)$

λ taper ratio $\left(\frac{\text{tip chord}}{\text{root chord}}\right)$

Λ angle of sweepback of the quarter-chord line, degrees

ν kinematic viscosity, square feet per second

METHOD

The method proposed in this report is essentially the same as that given in references 1 and 2 for unswept wings. In common with these methods, it is assumed that when section maximum lift is exceeded at a section of the wing, separation with its attendant effects will be evident. The major difference lies in the fact that the concepts of simple sweep theory (reference 3) are also incorporated to establish the maximum section lift coefficients across the wing. This theory shows that the significant airfoil section is that one lying normal to a swept reference line. It follows that the effective velocity is that component of free-stream velocity which is parallel to the significant airfoil section. When the effective velocity is used as a reference velocity, maximum lift coefficients of such swept sections can be taken directly from two-dimensional values. Since the free-stream velocity is used in deriving the force characteristics of swept wings, these two-dimensional maximum lift coefficients are also referred to this larger velocity when applied to a swept wing. Thus the resulting two-dimensional values are considerably reduced, accounting in large part for the low wing lift coefficients at which section stall first occurs on swept wings.

Three assumptions are involved in this use of simple sweep theory. First, although strictly applicable only to infinite-span yawed wings, the theory is herein assumed valid on finite-span swept wings to within a negligible distance of the root and tip sections. Second, the sweep of the quarter-chord line is assumed to be representative of the angle of sweep of tapered wings. These two assumptions are reasonable at wing lifts prior to the appearance of flow separation on the wing except for wings of low aspect ratio or taper ratio. Third, the simple $\cos \Lambda$ relation between free-stream velocity and the normal velocity component (which holds true when the pitching axis is parallel to the quarter-chord line) is used rather than the exact equations for a swept-back wing.

As in references 1 and 2, two-dimensional data are used to define the maximum lift of the significant airfoil sections. Data obtained at comparable Reynolds numbers are used, and this becomes of considerable

importance in the case of the swept wing where the reduced velocity often brings the operating Reynolds numbers of the sections into a critical range, even at full scale.

With the spanwise distribution of maximum section lift determined, references 4 and 5 are then used to define the span lift-coefficient distribution on the wing. As was done in references 1 and 2, this lift-coefficient distribution is adjusted until it becomes tangent to the line of maximum section lift coefficients. This point of tangency is taken to be the point of the first occurrence of section maximum lift on the wing, and the area under the curve of lift-coefficient distribution represents the wing lift coefficient above which the aerodynamic characteristics will show marked changes.

Example applications of this method will be given in another section of this report.

MODELS AND APPARATUS

The investigation of the swept-wing model was made in the Ames 40- by 80-foot wind tunnel. A three-view drawing of the model with its principal dimensions is given in figure 1; additional dimensional data are listed in table I. A view of the model mounted for testing in the wind tunnel is shown in figure 2.

The wing had an aspect ratio of 6, a taper ratio of 0.4, and an angle of sweepback of the 25-percent-chord line of 45°. The wing thickness distribution was that of an NACA 65-009 section modified by fairing straight lines from 66-percent chord to the trailing edge. This modified profile (table II) was applied normal to the wing 25-percent-chord line. The wing was attached in a high midwing position to a fuselage of fineness ratio 10.9. The wing was equipped with trailing-edge split flaps of 30-percent chord extending from the wing-fuselage juncture to 40-percent semispan. (See fig. 3(a).)

The stall-control devices and modifications to the wing consisted of upper-surface boundary-layer-control fences, a leading-edge flap, and an increased leading-edge radius. Details of these devices and modifications are given in figures 3, 4, and 5. The leading-edge flaps of 4.75-percent chord had a fixed deflection of 42°. The increased leading-edge radius was equal to that of the NACA 0012 airfoil section. It was fitted to the wing such that the upper wing surface remained essentially unchanged, and the added thickness was gradually faired into the lower wing surface; this introduced 0.42-percent camber into the modified profile.

Two-dimensional models of 2-foot chord of the three wing sections were made of mahogany and shellacked and sanded. They were equipped

with from 37 to 39 pressure orifices. The models completely spanned the width of a 2- by 5-foot open circuit wind tunnel in which they were tested.

TESTS

The test results presented for the swept-wing model are for a Reynolds number of approximately 9×10^6, based on the mean aerodynamic chord. This was at a dynamic pressure of approximately 48 pounds per square foot and at a Mach number of 0.2. Three-component force data were taken on all configurations, and tuft studies on several.

No lift, drag, or pitching-moment tares were applied to the data because the interference effects between the fuselage and the support fittings were unknown. A correction for stream-angle inclination was made. The tunnel-wall-interference corrections to the measured angles of attack and the drag coefficients were as follows:

$$\alpha_T = 0.60\ C_L$$

$$C_{D_T} = 0.010\ C_L^2$$

The two-dimensional tests were made at a Reynolds number of 2×10^6 and were comprised of pressure-distribution measurements and tuft studies. Section lift coefficients were determined from the pressure distributions according to the expression

$$c_l = c_n \cos \alpha_o - c_c \sin \alpha_o$$

Corrections for wind-tunnel-wall interference were not applied to the results.

DISCUSSION

Basic Model

A study was first made of the model without modifications in order to determine the validity of the procedure and to indicate what direction any geometric model changes should take to bring desired improvements. Two-dimensional tests of the original airfoil section showed a maximum lift coefficient of 0.92. Since the section was constant across the swept wing, this value was taken as the maximum attainable at any point on the wing. (It must be remembered that a difference in Reynolds number existed between two- and three-dimensional cases.) Referring this to free-stream velocity showed that when any section of the wing reached a lift coefficient of 0.46, that section

would be at its maximum lift and any further increase in wing lift would produce sudden changes in wing characteristics. The theoretical span lift-coefficient distribution (fig. 6) showed that the maximum section lift should be reached first at 73-percent semispan at a wing lift coefficient of 0.38; considering the longitudinal location of this section with respect to the moment center, a strong nose-up tendency would be anticipated above the wing lift coefficient of 0.38.

Force tests of the model showed, as anticipated, that noticeable force and moment changes occurred at a low wing lift coefficient (fig. 7). The drag rise increased abruptly at about 0.5 lift coefficient; the pitching moment increased negatively between 0.50 and 0.55 lift coefficient before giving evidence of a strong nose-up moment. It could be concluded from conservativeness of the predicted value (0.38) either that maximum lift must be exceeded over an appreciable wing area before large changes in forces occur or, and it is believed this is more likely, that three-dimensional effects which are not considered in this analysis, such as induced section camber and boundary-layer flow, enable sections to reach higher than two-dimensional maximum lift.

Effects of split flaps.- A similar analysis and comparison with experiment was made for the unmodified wing with split flaps deflected 15°, 30°, and 45°. No two-dimensional data for the wing section with a split flap were available, hence estimates of section $(\Delta\alpha/\Delta\delta_f)_{c_l}$ (necessary when using reference 5 to obtain span-load distributions) and section maximum lift coefficient were made from other data;[1] values of 0.39, 0.34, and 0.30 were used for flaps deflected 15°, 30°, and 45°, respectively. The maximum section lift coefficients selected for the three flap deflections were 1.32, 1.52, and 1.70. The three-dimensional wing was therefore assumed to have a section maximum lift, based on free-stream velocity, of 0.66, 0.76, or 0.85 extending from the inboard to the outboard edges of the flaps and, as before, 0.46 over the remainder of the span.

Since the basic lift distribution due to a given flap deflection remains constant for all wing lifts prior to the occurrence of section maximum lift on the wing, it is suggested in reference 2 that this portion of the theoretical lift distribution be subtracted from the line of maximum section lifts. This new line defines the maximum allowable additional-lift distribution, and the theoretical additional-lift distribution is easily adjusted to become tangent to it. This value of theoretical additional lift is then the predicted wing lift for the first occurrence of section maximum lift. Application of this procedure shows that just inboard of the outboard extent of the flap very high additional lift can be carried and just outboard very little can be

[1]This form of the lift-effectiveness parameter is used rather than $d\alpha/d\delta_f$ since the flap deflections of interest herein exceed the range where $d\alpha/d\delta_f$ is constant.

carried. (See fig. 8(a).) In reference 2, it is further suggested that in the latter region the extreme variation in allowable additional lift be ignored and that a smooth fairing be made between the inboard and outboard allowable lift distributions. In the case of straight wings, this fairing is fairly simple since the inboard and outboard allowable additional lift distributions are at about the same level and the indeterminate region is quite short. In effect, this fairing means that the maximum lifts of the flapped sections near the flap extremities are being arbitrarily reduced and those of the unflapped sections near the flap extremities are being arbitrarily increased.

In the case of swept wings, the foregoing procedure could not be applied readily. Figure 8(b) shows that the different basic load distribution due to flaps on swept wings resulted in a condition where a wide range of possible fairings existed. It was evident that a better estimation of the lift limits was required in this region. The assumption was therefore made that the maximum lift of the sections outboard of the flaps would be increased an amount equal to the increment of loading induced on the sections by the flaps. Such an assumption was believed to be acceptable since analysis shows that flaps induce primarily a camber-type loading on adjoining sections, and two-dimensional tests show that for moderate amounts of camber maximum lift is increased by an amount equal to the camber lift. For the flapped sections the maximum lift was retained as that found by two-dimensional tests. Proceeding on this basis a new distribution of maximum section lifts was defined. The spanwise distribution of section lift coefficient was then found for each flap deflection which was tangent at some point to the maximum lift-coefficient distribution (e.g., fig. 9).

The predicted wing lift coefficients at which section stall first occurred were 0.47, 0.54, and 0.62 for 15°, 30°, and 45° flap deflection. The corresponding measured wing lift coefficients at which marked force and moment changes occurred (fig. 7) were 0.58, 0.60, and 0.62. (It must be noted here that double fences were on the wing for these tests but, as will be discussed later, it was felt that these fences had little or no effect on the wing lift coefficient at which section stall first occurred.)

It should be pointed out that such flaps as used here are not well suited to swept wings that have lift-coefficient distributions similar to that described herein. Much of the wing was well below its maximum lift when the first section stalled. To move the point of initial occurrence of section maximum lift well inboard (nose-down pitching moment) and, at the same time, to have all sections approaching their maximum lift together, it would be necessary to use flaps having larger effectiveness in relation to their maximum lift.

Effects of leading-edge modifications.- Study of the two-dimensional data on the original wing section showed that the section reached $c_{l_{max}}$ because of separation of flow from the leading edge

which in turn resulted from excessive peak pressures at the leading edge. Two modifications were designed to reduce this leading-edge pressure peak and thus increase $c_{l_{max}}$. Comparative pressure distributions in figure 10 for the three sections show the extent to which the peak pressure was reduced and the lift curves in figure 11 show the increase in $c_{l_{max}}$.

Each of the two modifications was tested on the swept-wing model as a full-span modification and with the trailing-edge flaps set at 0° and 15°. The leading-edge flap was also tested as a partial-span installation extending from the tip to 70-percent semispan in one case and from the tip to 40-percent semispan in a second case.

Predictions of the wing lift coefficient and of the spanwise location at which a section first reached maximum lift were made for each of the modified-wing conditions. The procedure followed was identical to that already discussed in detail. It should be noted, however, that it was assumed the partial-span leading-edge flaps raised the maximum lift only of the sections of the wing on which they were installed and, unlike the trailing-edge flaps, did not affect the maximum lift of the remainder of the wing. Examples of the spanwise distributions of maximum section lift coefficient and of lift coefficient which were used to make these predictions are shown in figure 12. The force test results, from which were chosen the wing lift coefficients for section maximum lift, are shown in figure 13. Table III summarizes the comparisons of the predicted and measured results on all configurations.

Compared with experiment, the predictions are conservative, and to about the same degree as found for the unmodified wing with equal flap deflections. The lift increments due to the leading-edge modifications are predicted with good accuracy in most cases. This indicates that no great change occurred in the magnitude of the unaccounted for three-dimensional effects.

Effects of fences.- Wing fences are designed to obstruct the spanwise flow of boundary-layer air on the wing upper surface and thereby prevent excessive thickening of the boundary layer in the tip regions with a resultant delay in flow separation over this critical area. Tests were made on the subject model of fences which had proved effective at small scale. Analysis such as proposed herein would, of course, indicate that fences would have no effect on the initial occurrence of maximum lift on a section of the wing. Such generally proved to be the case (figs. 7 and 14) although tufts indicated local areas of separation at very low wing lift coefficients (fig. 15) which were not present when the wing was at the same lift coefficients but was without fences. The fences showed some effect on the wing pitching moment at wing lift coefficients above that for first section stall, but in contrast to small-scale results, the pitching moment was erratic and only slightly less unstable. It must be noted that in cases where wing fences prove

effective in delaying the occurrence of flow separation, the proposed procedure will not account for their effect.

Application to Other Plan Forms

As a check of the validity of the method of this report over various combinations of sweep angles, aspect ratios, and taper ratios, a brief study was made of a limited number of other wing designs. The comparisons of the predicted and measured values of wing lift coefficient for initial section stall for these wings are given in table IV. The force and moment characteristics from which the measured values were chosen are reproduced in figure 16. The test results presented in figure 16 were taken from references 6, 7, and 8 and from unpublished data of the Ames 40- by 80-foot wind tunnel. In general, the comparisons of measured and predicted values show the same degree of accuracy of the method as was found in its application to the model tested for this report.

CONCLUDING REMARKS

The method outlined herein, which combines the concepts of simple sweep theory and swept-wing span-loading theory, provides a means of obtaining a quantitative estimate of the wing lift coefficient at which section maximum lift is first attained on a swept wing. This wing lift coefficient is generally equal to or slightly less than that at which marked changes in some or all of the over-all wing characteristics occur.

Evaluation of the method by comparison with experimental data from tests of a particular design showed that, for the conditions studied, the method was conservative in that it predicted the first occurrence of section stall at a wing lift coefficient usually 0.1 to 0.2 lower than that indicated by changes in force characteristics. However, because the discrepancies were consistent for the leading-edge modifications, the method usually predicted quite accurately the incremental gains due to these modifications.

Ames Aeronautical Laboratory
National Advisory Committee for Aeronautics,
Moffett Field, Calif.

REFERENCES

1. Anderson, Raymond F.: Determination of the Characteristics of Tapered Wings. NACA Rep. 572, 1936.

2. Pearson, Henry A., and Anderson, Raymond F.: Calculation of the Aerodynamic Characteristics of Tapered Wings with Partial-Span Flaps. NACA Rep. 665, 1939.

3. Jones, Robert T.: Effects of Sweepback on Boundary Layer and Separation. NACA Rep. 884, 1947. (Formerly NACA TN 1402)

4. DeYoung, John, and Harper, Charles W.: Theoretical Symmetric Span Loading at Subsonic Speeds for Wings Having Arbitrary Plan Form. NACA Rep. 921, 1948. (Formerly NACA TN's 1476, 1491, and 1772)

5. DeYoung, John: Theoretical Symmetric Span Loading Due to Flap Deflection for Wings of Arbitrary Plan Form at Subsonic Speeds. NACA TN 2278, 1951.

6. McCormack, Gerald M., and Cook, Woodrow L.: A Study of Stall Phenomena on a 45° Swept-Forward Wing. NACA TN 1797, 1949.

7. Letko, William, and Feigenbaum, David: Wind-Tunnel Investigation of Split Trailing-Edge Lift and Trim Flaps on a Tapered Wing With 23° Sweepback. NACA TN 1352, 1947.

8. Hunton, Lynn W.: Effects of Twist and Camber on the Low-Speed Characteristics of a Large-Scale 45° Swept-Back Wing. NACA RM A50A10, 1950.

TABLE I.- GEOMETRIC DATA OF THE MODEL

Wing	
Span, feet	42.26
Area, square feet	300
Mean aerodynamic chord, feet	7.512
Angle of incidence, degrees	0
Aspect ratio	6
Taper ratio	0.4
Sweepback of 25-percent-chord line, degrees	45
Fuselage	
Length, feet	52.67
Maximum diameter, feet	4.83

TABLE II.- COORDINATES OF THE MODIFIED NACA 65-009 AIRFOIL SECTION

[Percent of airfoil chord]

Station	Ordinate
0	0
.50	.700
.75	.845
1.25	1.058
2.50	1.421
5.00	1.961
7.50	2.383
10.00	2.736
15.00	3.299
20.00	3.727
25.00	4.050
30.00	4.282
35.00	4.431
40.00	4.496
45.00	4.469
50.00	4.336
55.00	4.086
60.00	3.743
65.00	3.328
[a]66.00	3.241
100.00	0
L.E. radius = 0.552	

[a]Section faired from 66-percent chord to the trailing edge by straight lines.

TABLE III.- COMPARISON OF PREDICTED AND MEASURED WING LIFT COEFFICIENTS FOR INITIAL SECTION STALL

Configuration	δ_f (deg)	Wing lift coefficient		η for initial stall
		Predicted	Measured	
Basic wing section	0	0.38	0.50	0.73
Basic wing section	15	.47	.58	.73
Basic wing section	30	.54	.60	.73
Basic wing section	45	.62	.62	.73
30-percent-span leading-edge flaps	0	.39	.55	.70
30-percent-span leading-edge flaps	15	.48	.63	.70
60-percent-span leading-edge flaps	0	.44	.62	.40
60-percent-span leading-edge flaps	15	.58	.72	.40
Full-span leading-edge flaps	0	.73	.90	.73
Full-span leading-edge flaps	15	.82	1.05	.73
Increased leading-edge radius	0	.56	.78	.73
Increased leading-edge radius	15	.65	.85	.73

TABLE IV.- COMPARISON OF PREDICTED AND MEASURED WING LIFT COEFFICIENTS FOR INITIAL SECTION STALL ON WINGS WITH VARIOUS PLAN FORMS

Aspect ratio	Taper ratio	Sweep angle, (deg)	Wing twist (deg)	Airfoil section	Wing lift coefficient		η for initial stall
					Predicted	Measured	
3.55	0.5	-45	0	NACA 64A112	0.68	0.60	0.15
7.51	.24	23	-4	NACA 4418	1.02	1.10	.74
4.8	.5	35	-2	NACA 0011-64 (modified)	.74	.87	.64
4.8	.5	35	-2	NACA 0011-64 (modified) $c_{l_i} = 0.38$	.99	1.22	.64
6	.5	45	-10	NACA 64A810, a = 0.8	.74	.83	.36
3.5	.25	60	0	NACA 64A010.5 (modified)	.20	.22	.75

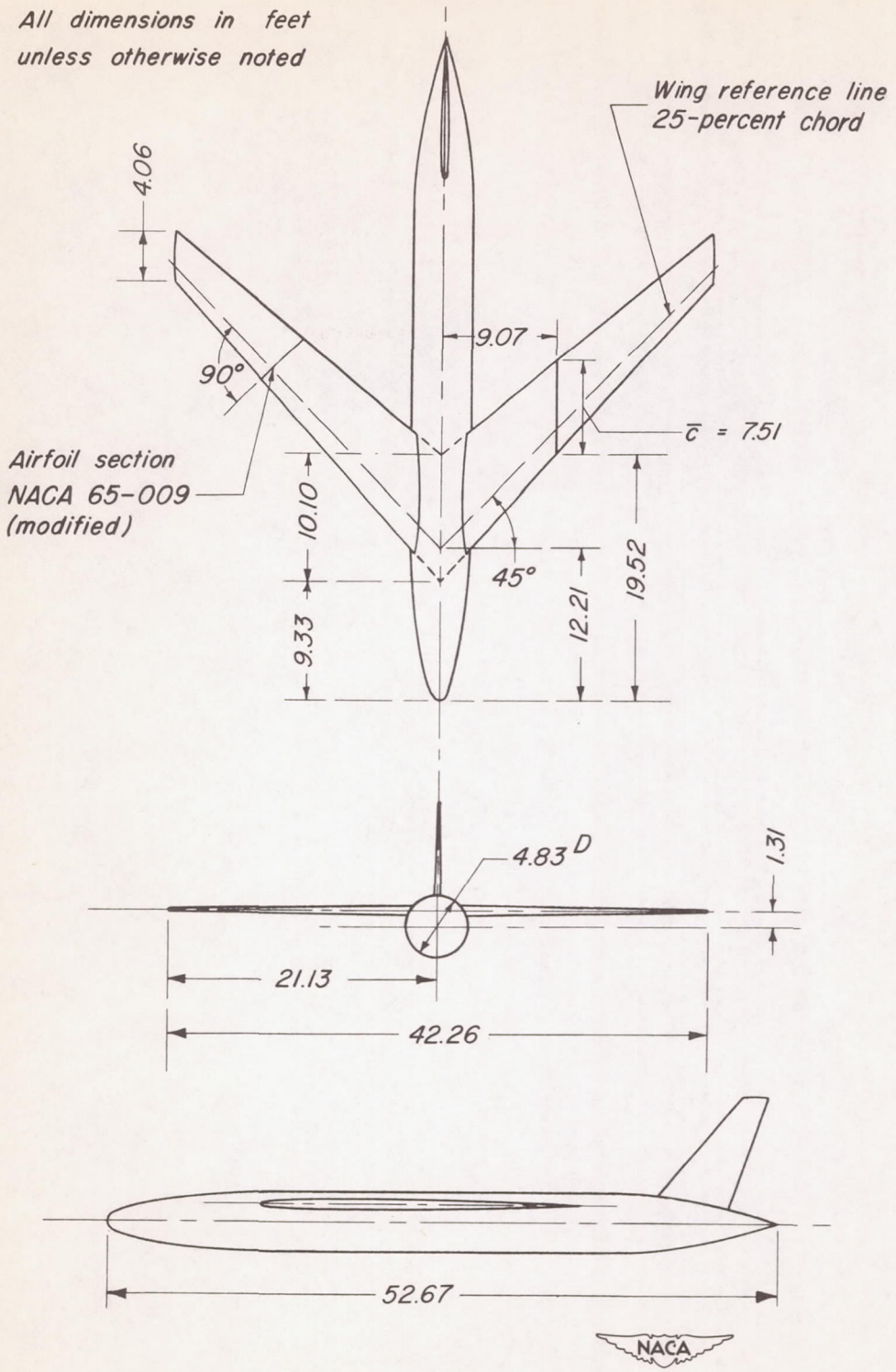

Figure 1.– Three-view drawing of the model.

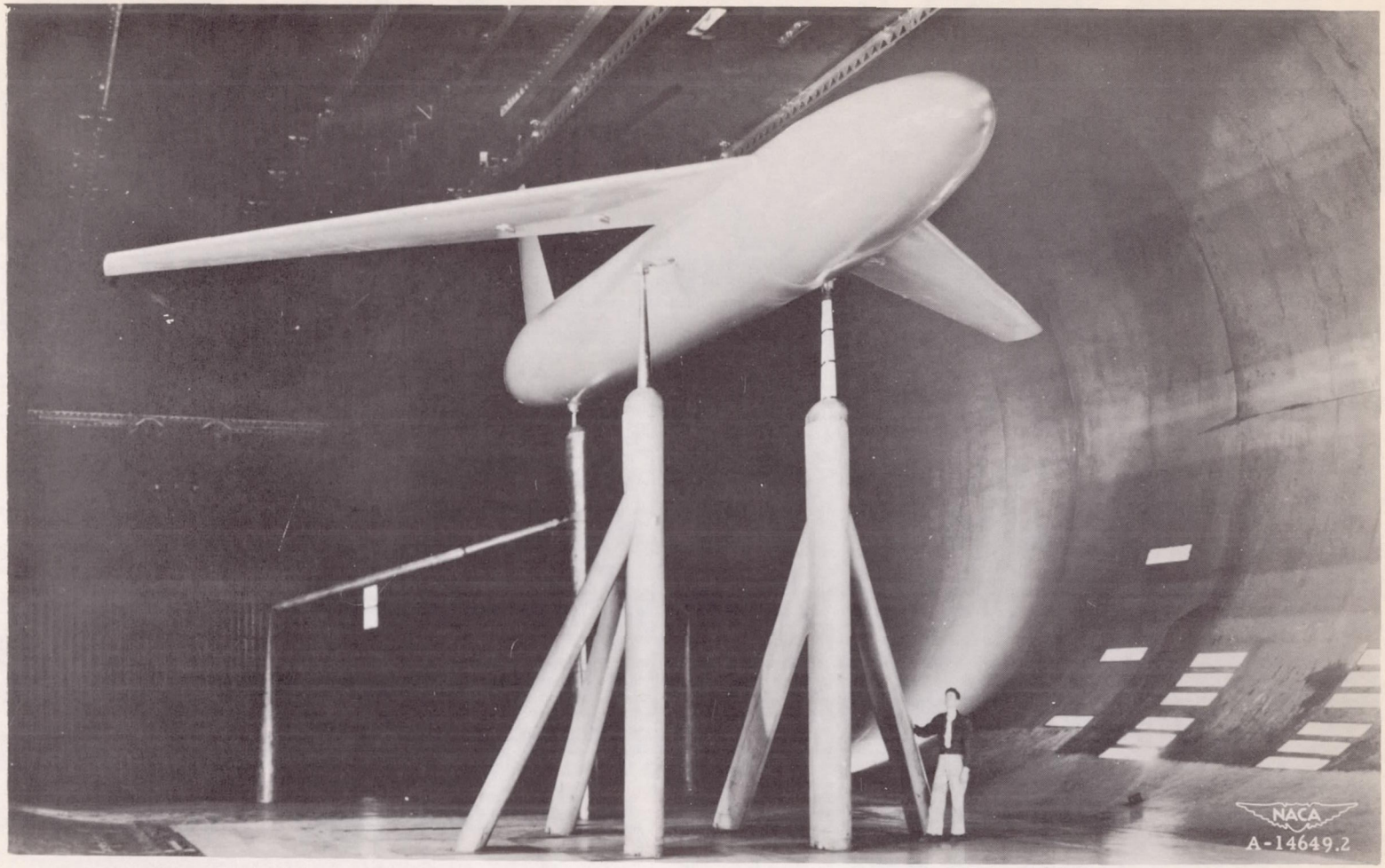

Figure 2.- General view of the model installed in the Ames 40- by 80-foot wind tunnel.

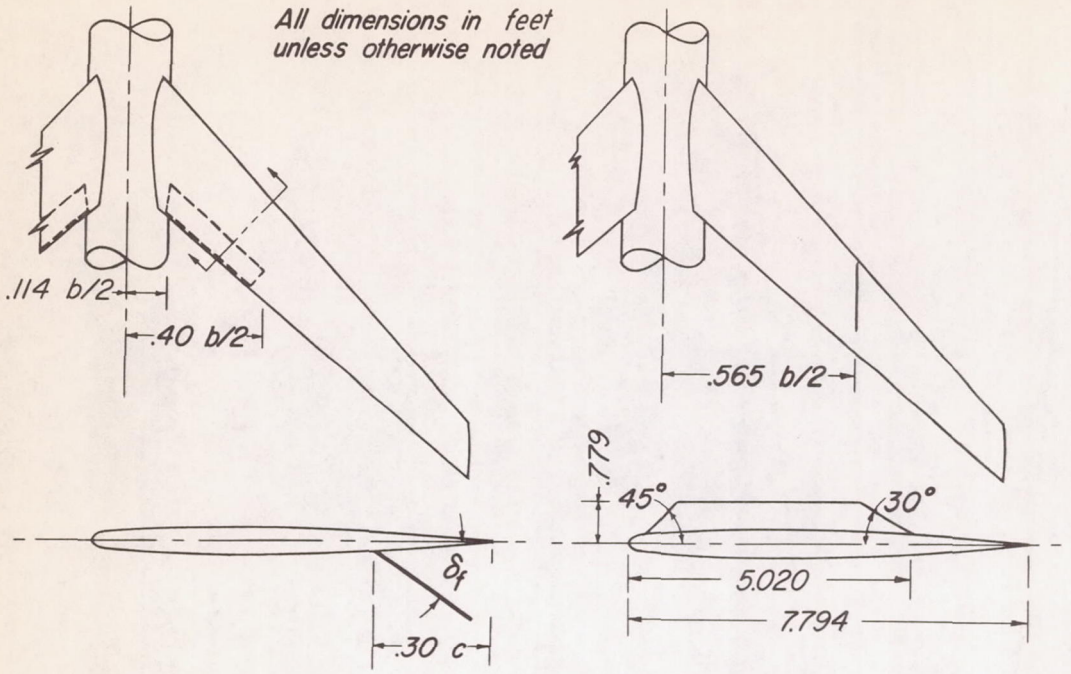

(a) Trailing-edge split flap.

(b) Single fence.

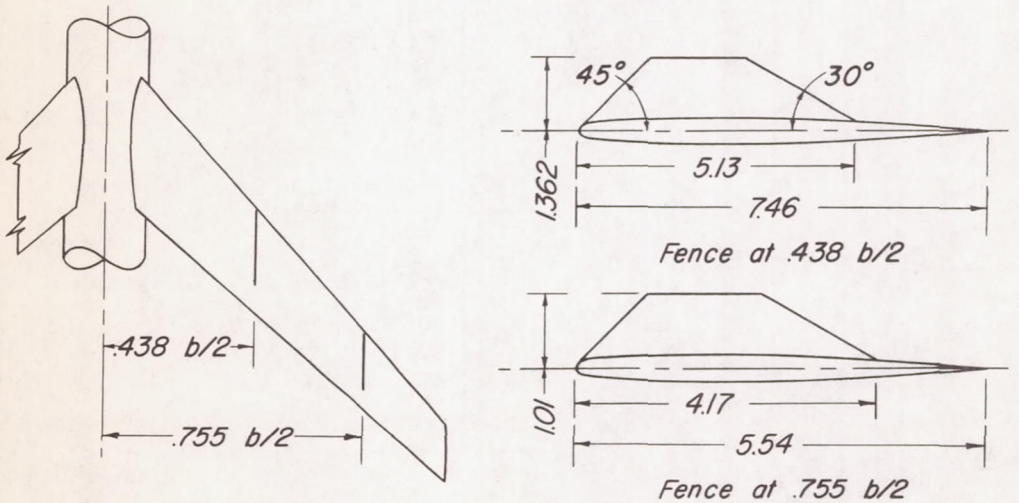

(c) Double fences.

Figure 3.- Details of the trailing-edge split flaps and the single and double fences.

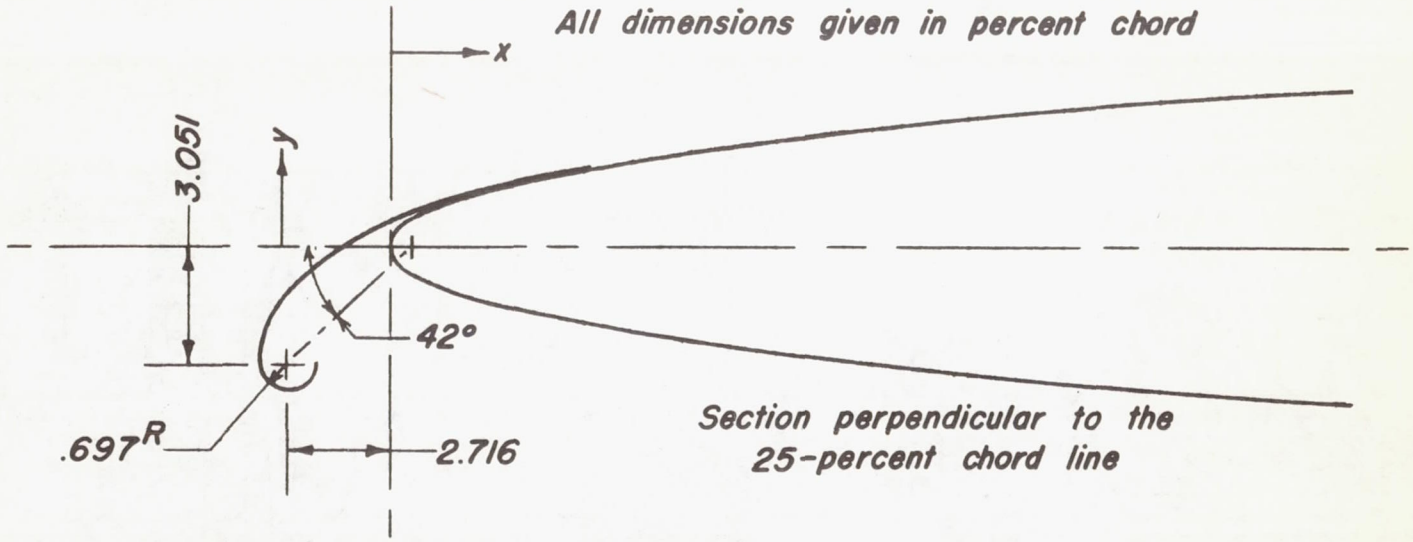

Coordinates

x	y	x	y
-3.443	-2.833	0	.669
-3.341	-2.339	.727	.959
-2.978	-1.584	1.453	1.221
-2.615	-1.118	2.180	1.424
-2.252	- .741	2.906	1.600
-1.888	- .435	3.633	1.743
-1.162	.065	4.358	1.874
- .435	.465	5.085	1.998

Figure 4. – Details of the leading-edge flap.

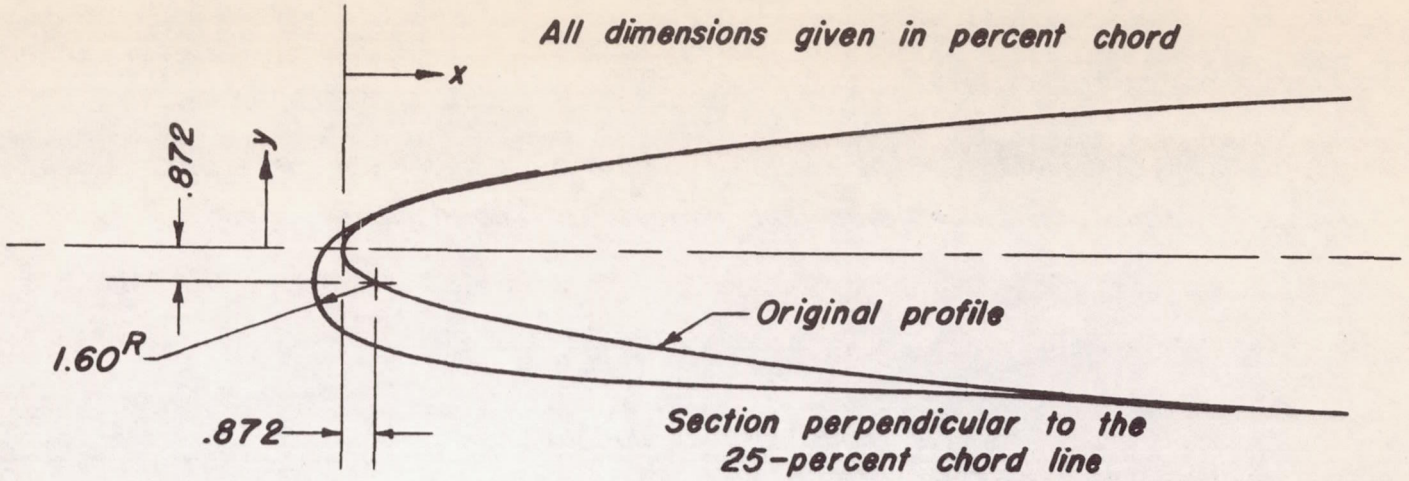

Coordinates

x	y_{upper}	y_{lower}	x	y_{lower}
-0.727	-0.872	-0.872	6.538	-3.305
- .362	.145	-1.816	7.991	-3.385
0	.465	-2.136	10.171	-3.458
.363	.697	-2.339	12.349	-3.508
.727	.886	-2.477	14.529	-3.537
1.453	1.191	-2.674	16.708	-3.596
2.180	1.387	-2.826	18.888	-3.719
3.633	1.729	-3.065	21.068	-3.865
5.085	2.005	-3.219	23.246	-3.981

Figure 5.– Details of the increased leading-edge radius.

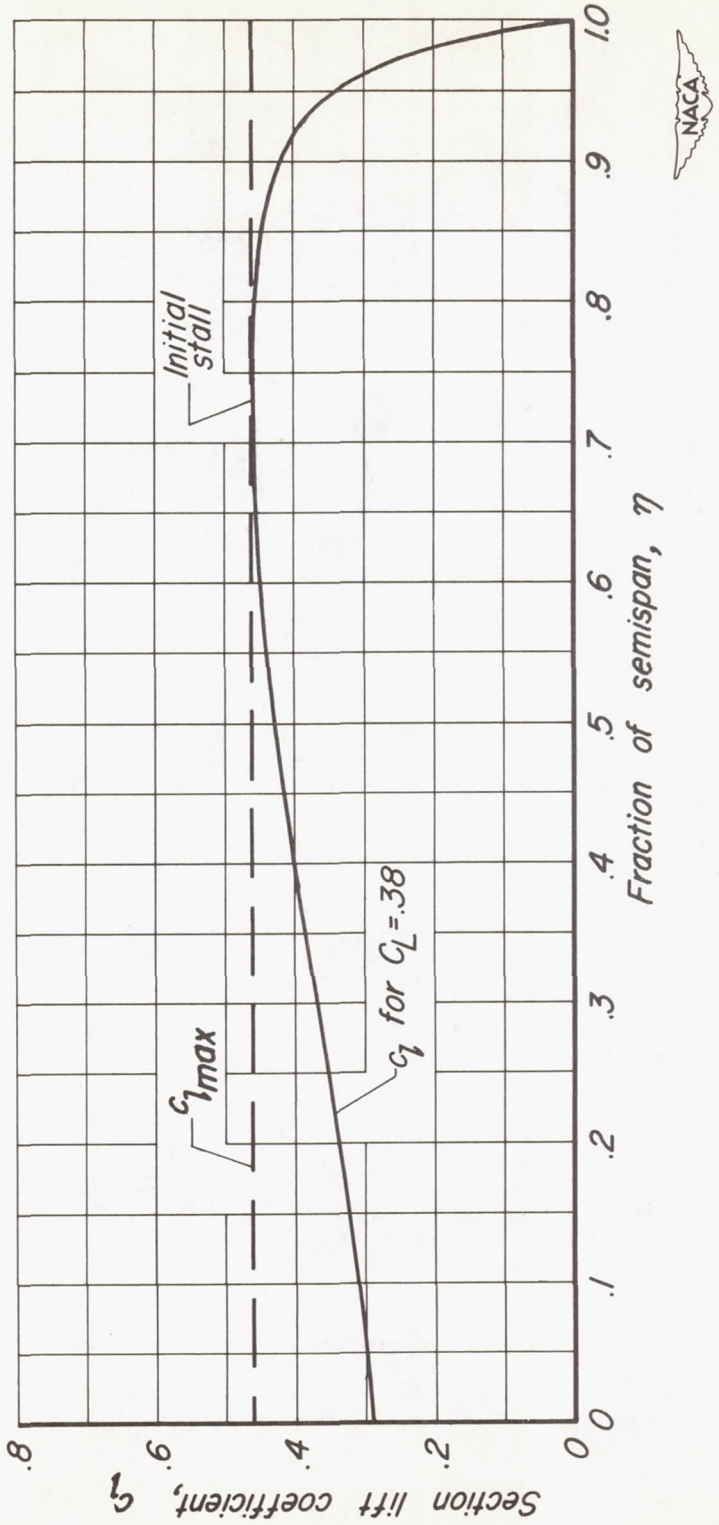

Figure 6.- Span distribution of section lift coefficient for initial section stall on the model without trailing-edge flaps.

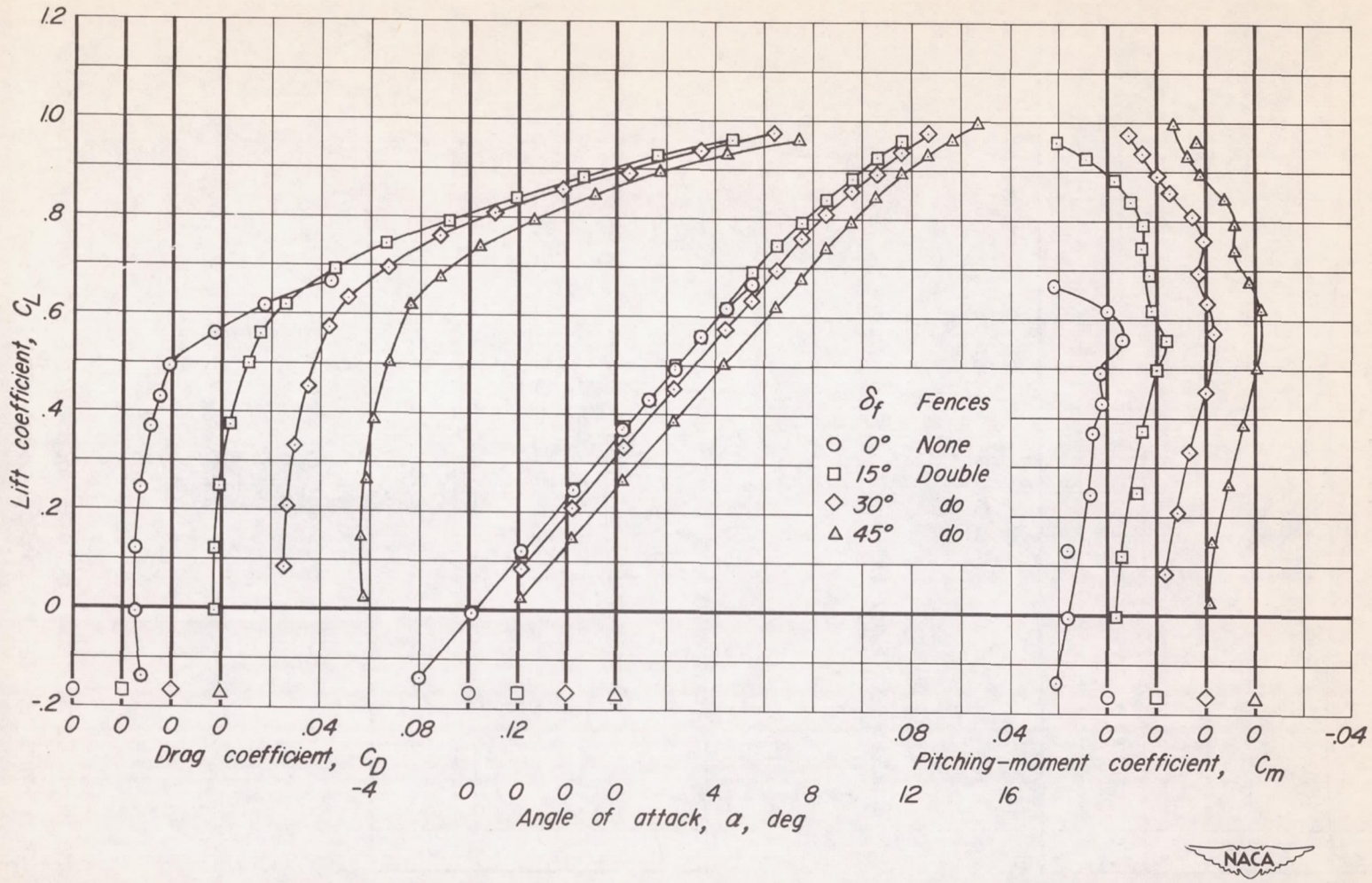

Figure 7. – Aerodynamic characteristics of the model with and without trailing-edge flaps; R, 9×10^6.

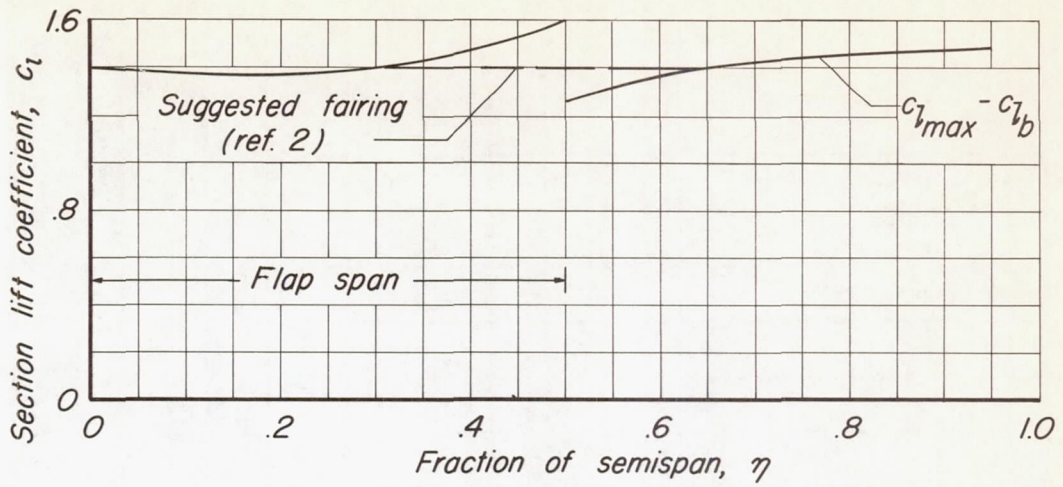

(a) Typical additional-lift limit for a flapped straight wing.

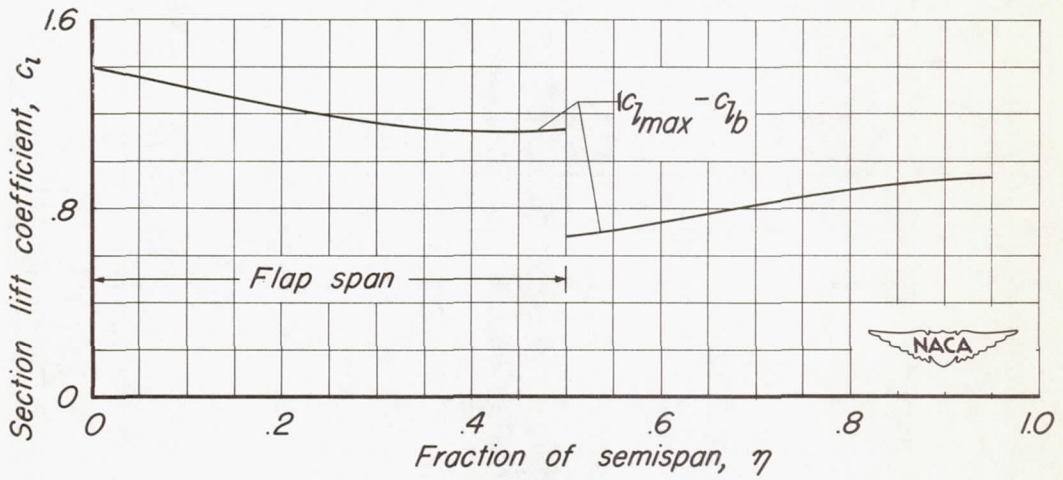

(b) Typical additional-lift limit for a flapped swept wing.

Figure 8.- Comparison of the application of the procedure of reference 2 to a straight wing and a swept wing.

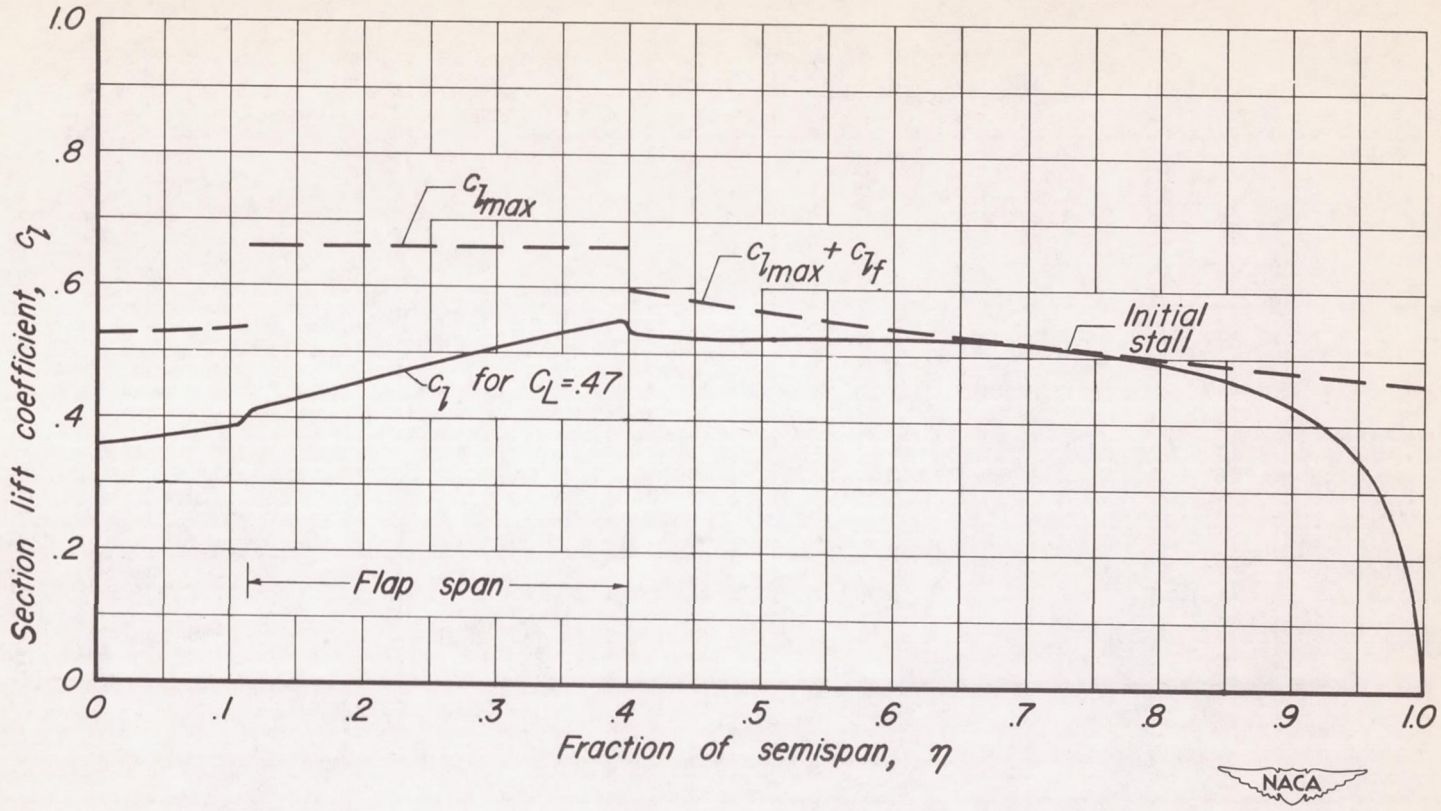

Figure 9. – Span distribution of section lift coefficient for initial section stall on the model with trailing-edge flaps deflected 15°.

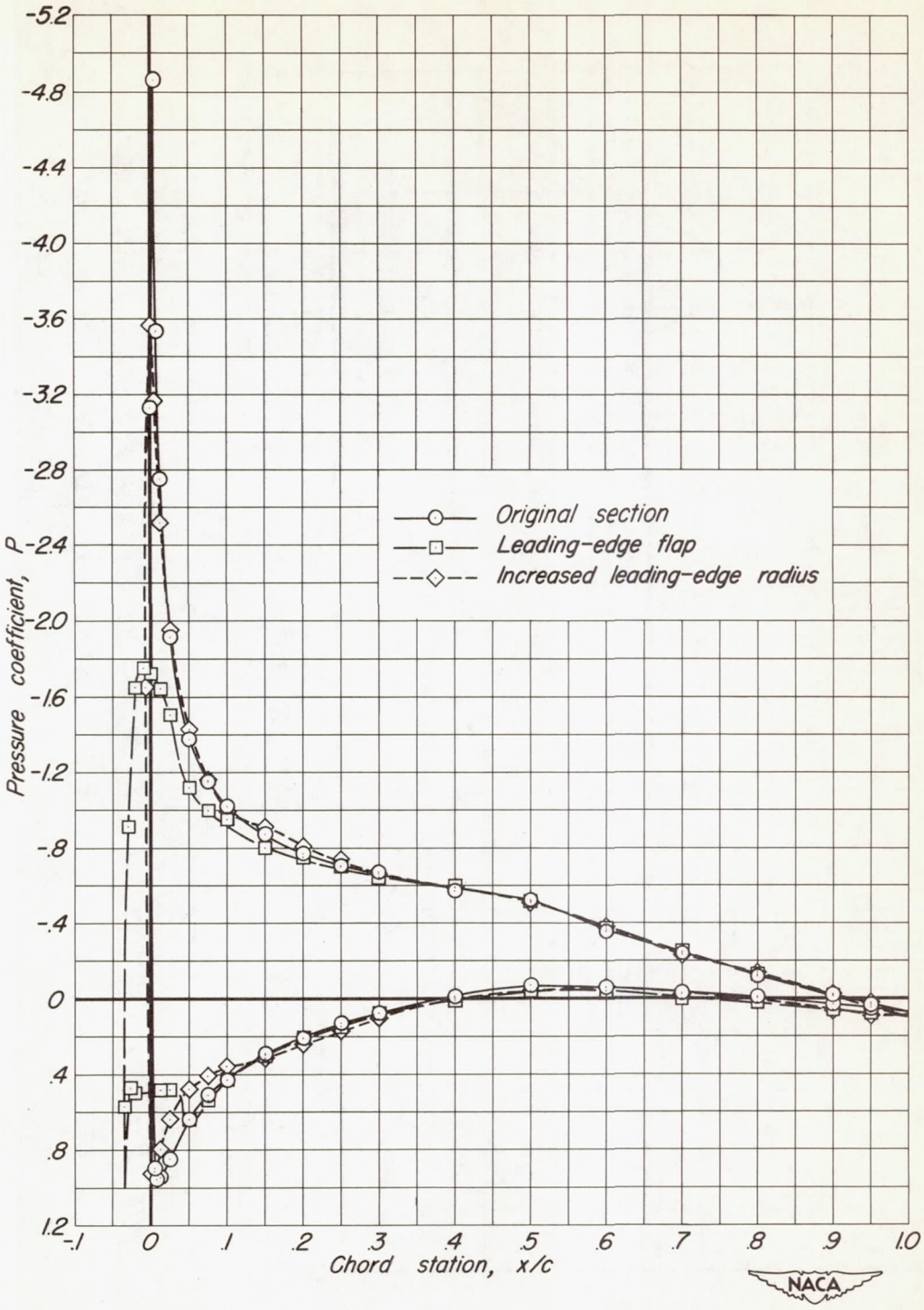

Figure 10.– Pressure distributions on the two-dimensional models at a lift coefficient of approximately 0.7 .

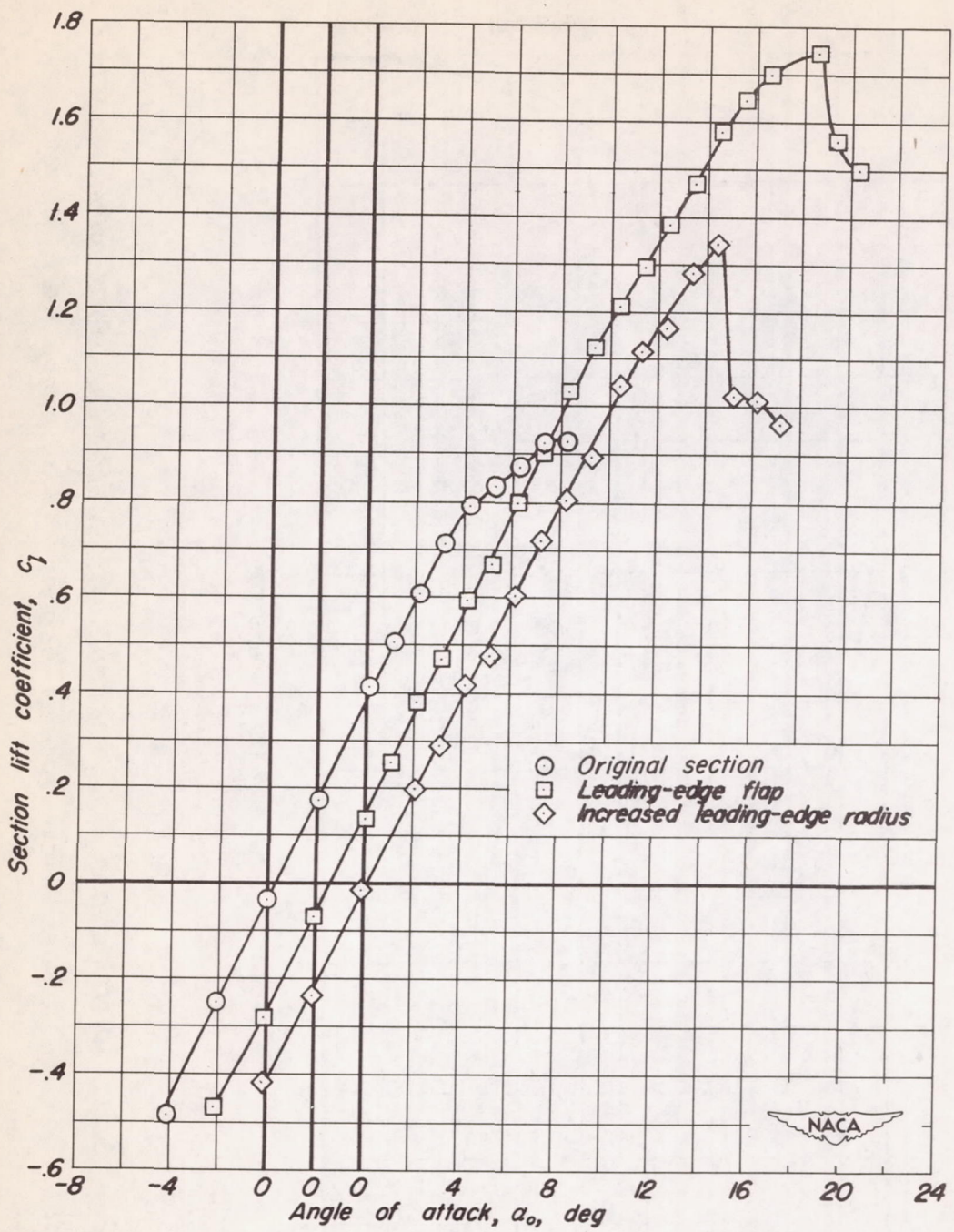

Figure 11.– Section lift curves for the two-dimensional models; R, 2.1×10^6.

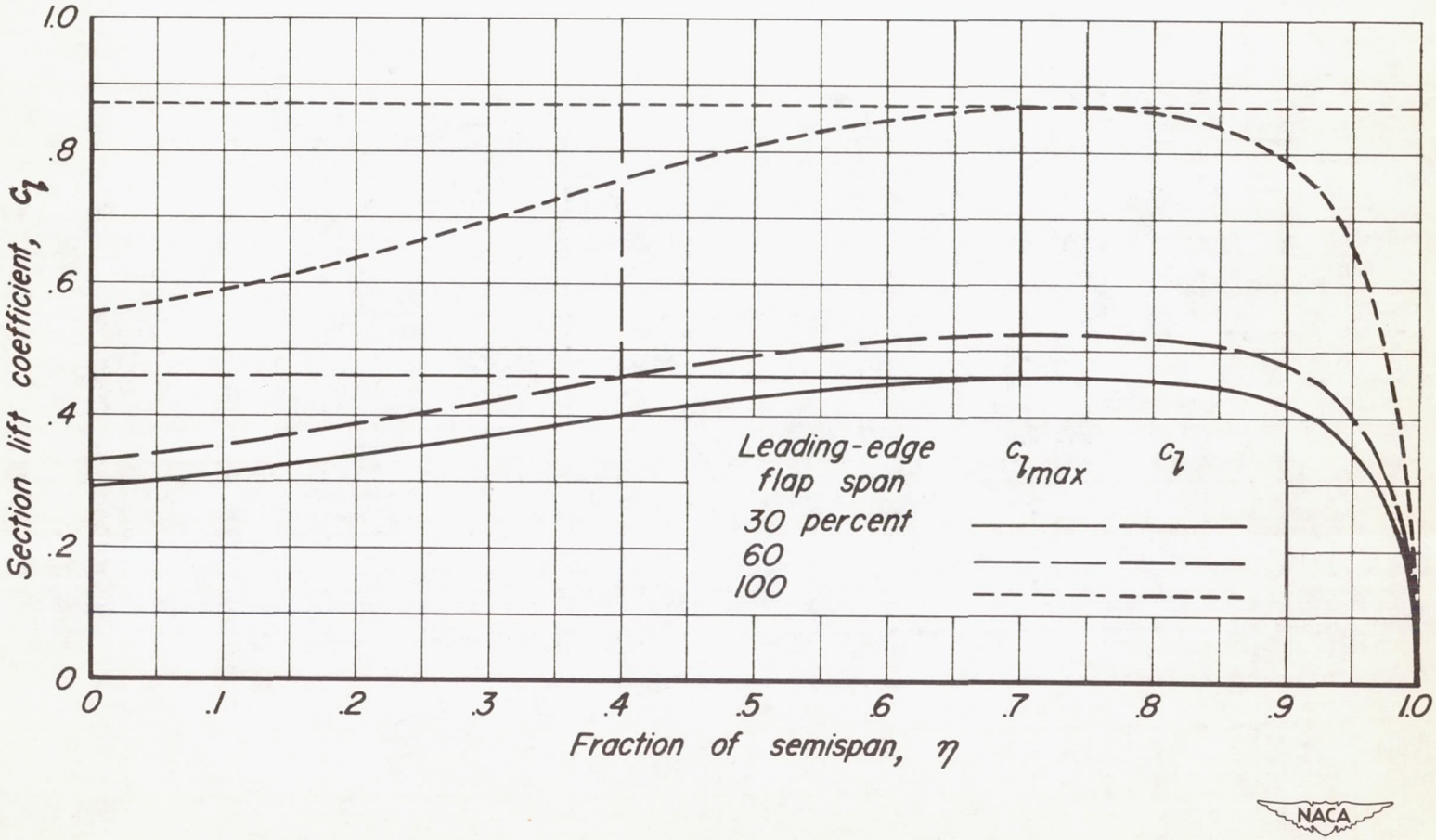

Figure 12.– Span distributions of section lift coefficient for initial section stall on the model with various spans of leading-edge flaps.

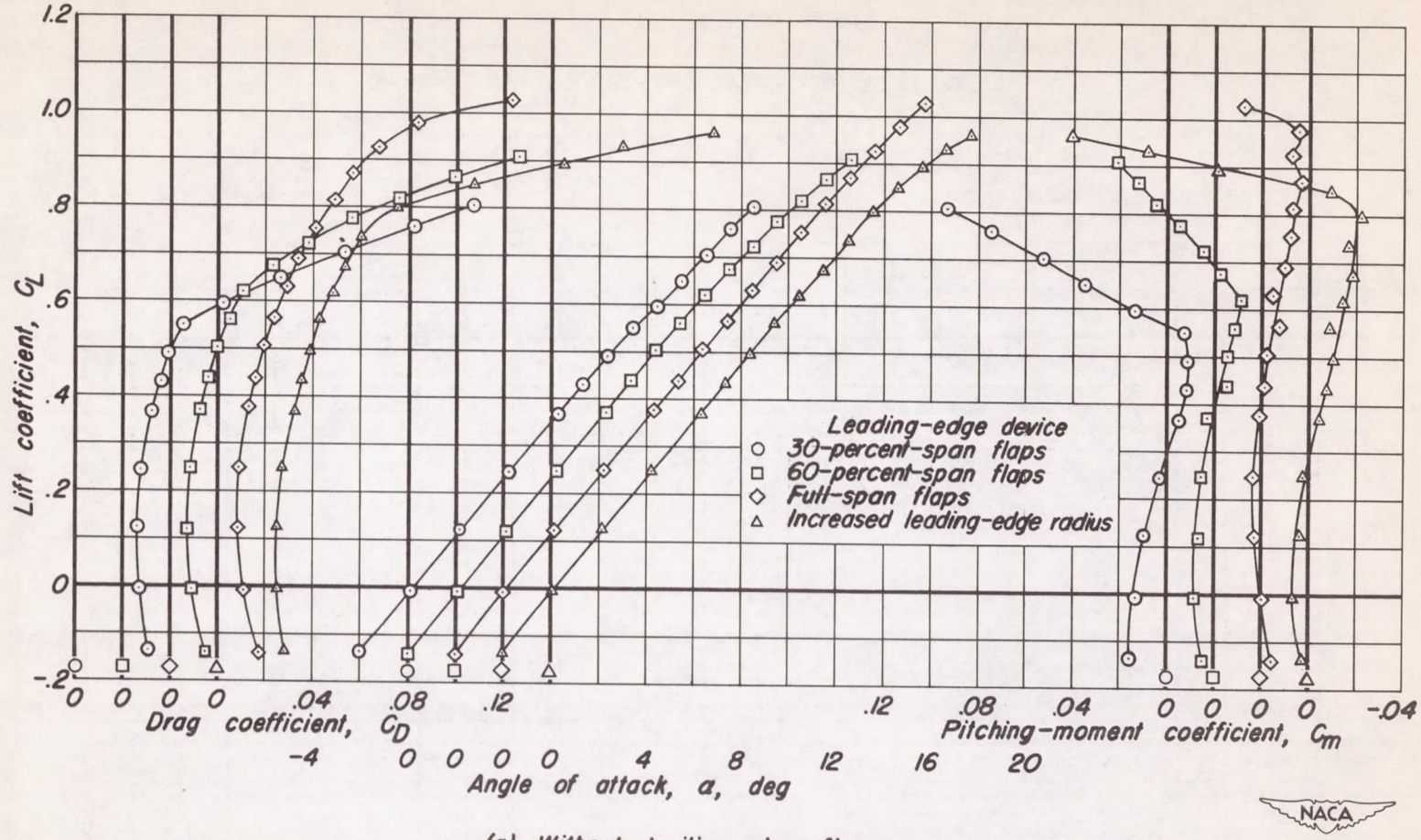

(a) Without trailing-edge flaps.

Figure 13. – Aerodynamic characteristics of the model with various leading-edge devices; R, 9×10^6.

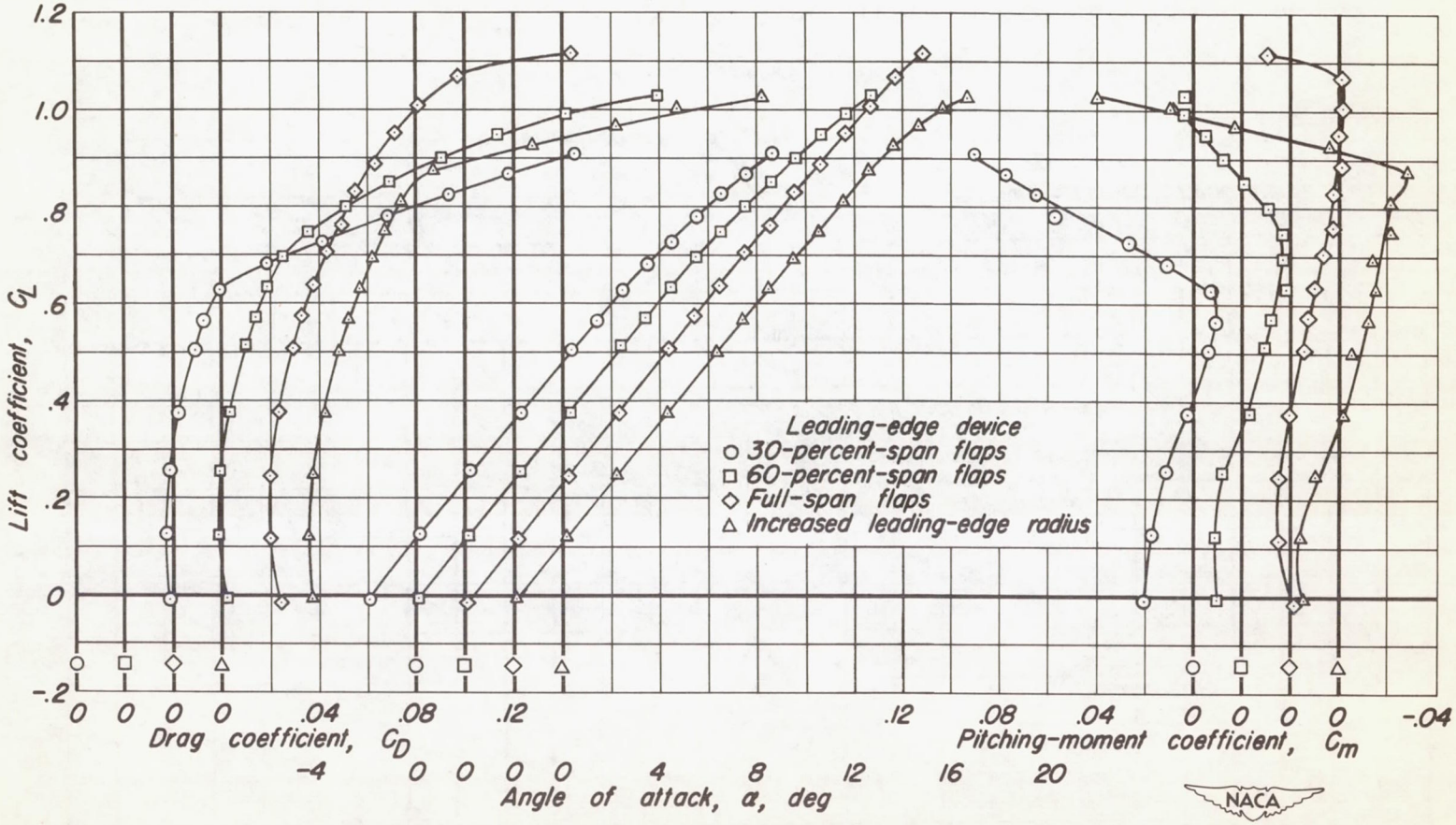

(b) Trailing-edge flaps deflected 15°.

Figure 13. - Concluded.

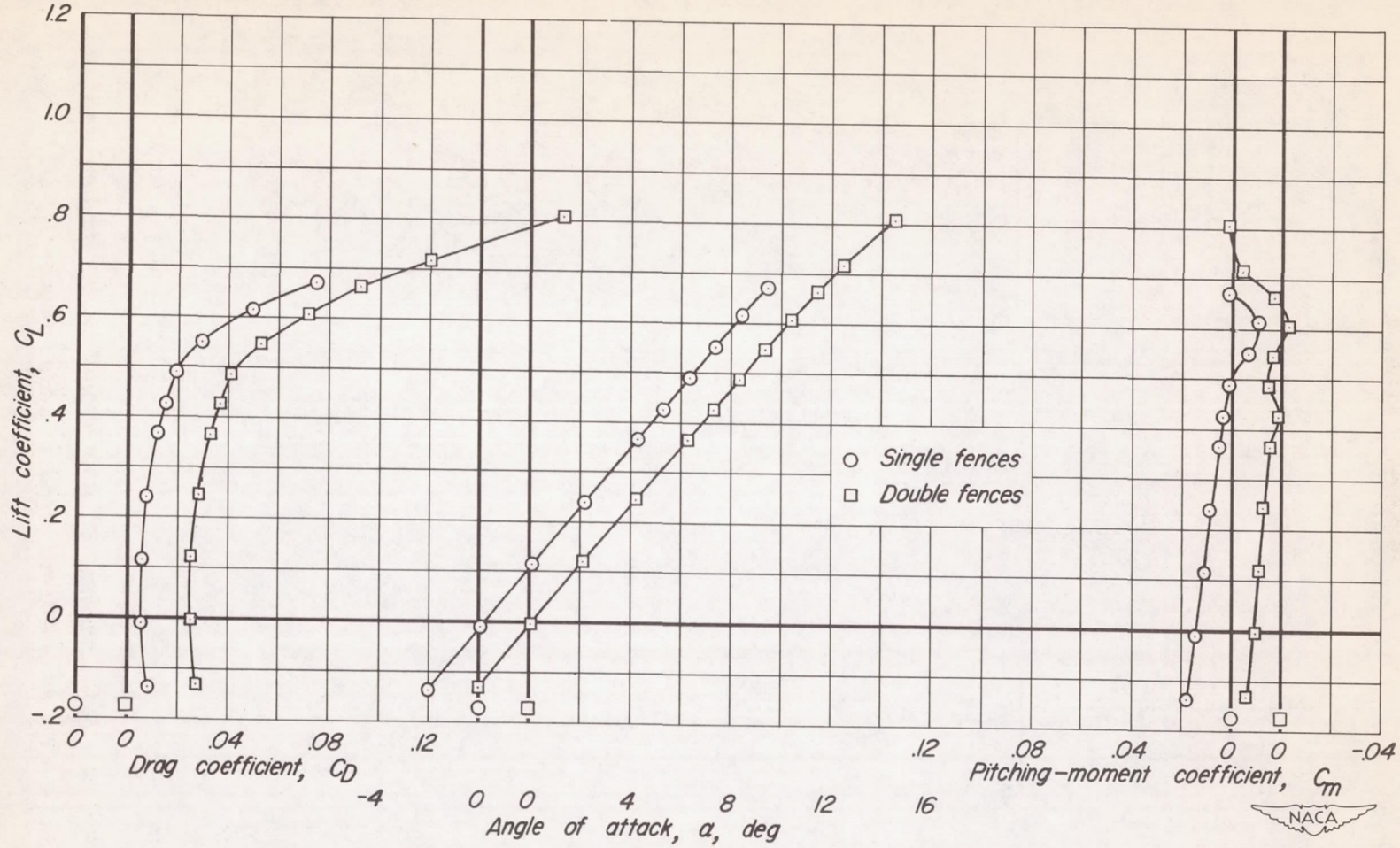

Figure 14. - Aerodynamic characteristics of the model with single and double fences. Without trailing-edge flaps; R, 9×10^6.

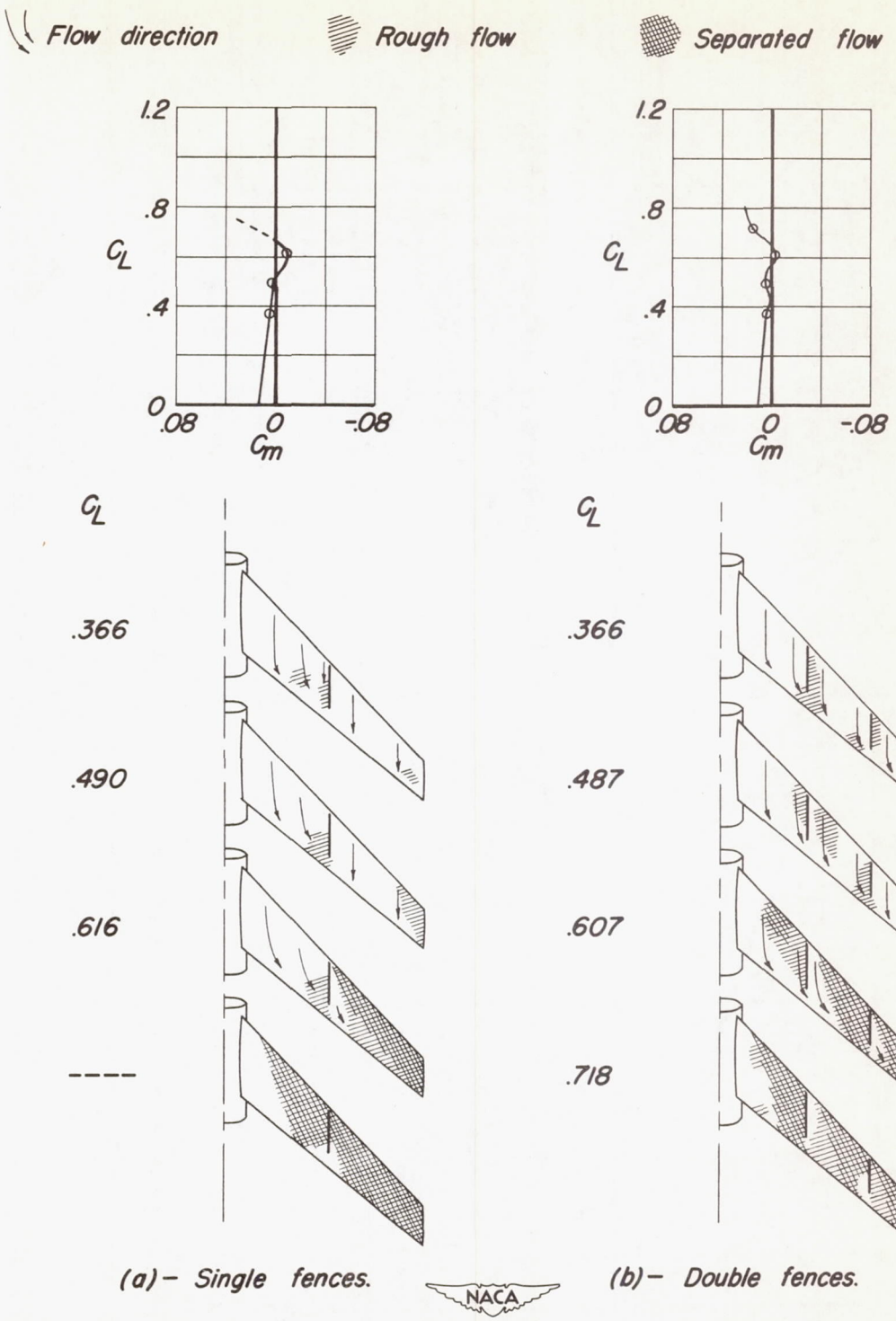

(a)– Single fences. (b)– Double fences.

Figure 15.—Tuft studies of the model with single and double fences. Without trailing-edge flaps; R, 9×10^6.

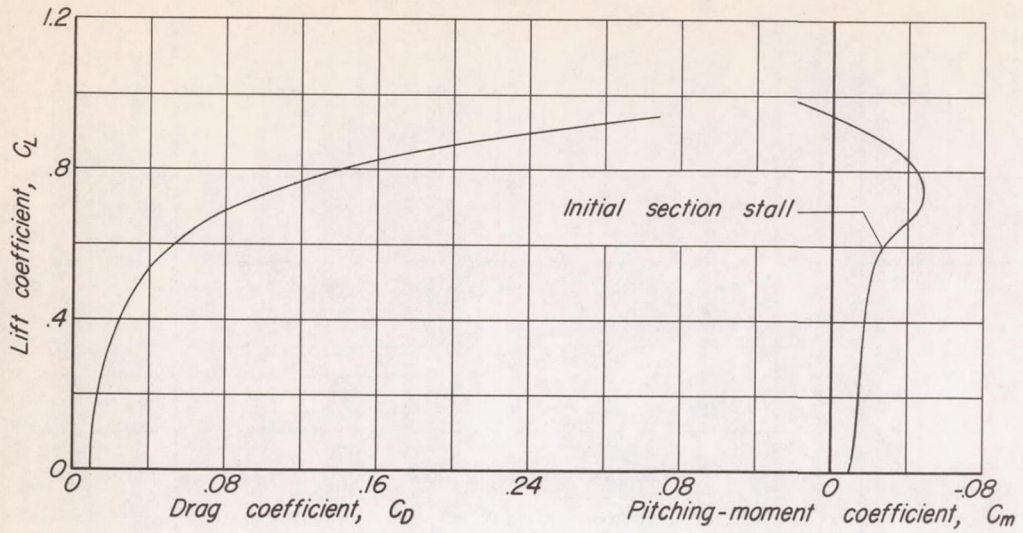

(a) Wing of reference 6. A, 3.55; λ, .5; Λ, -45°.

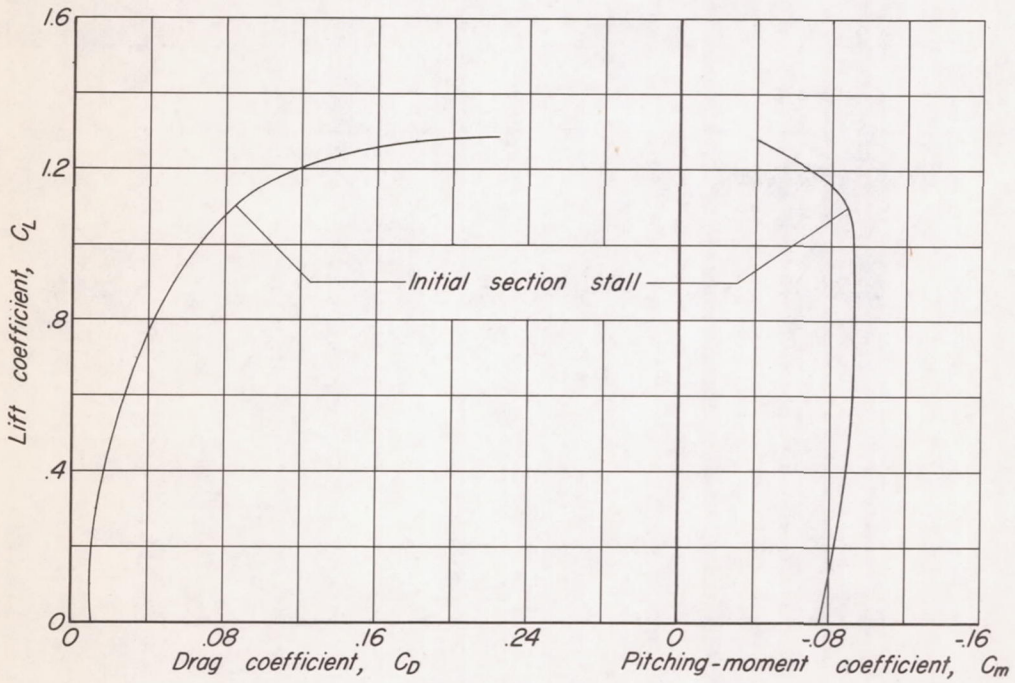

(b) Wing of reference 7. A, 7.51; λ, .24; Λ, 23°.

Figure 16.- Force and moment characteristics for wings of various plan forms from which wing lift coefficients for initial section stall were chosen.

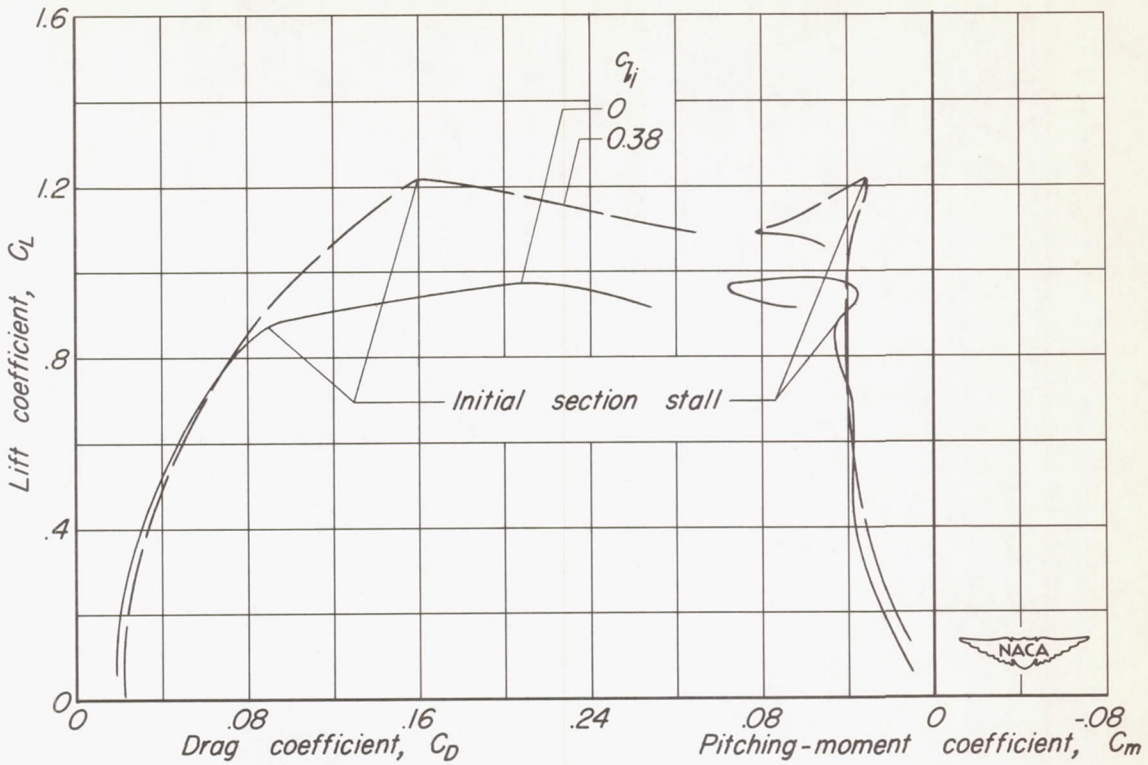

(c) Data from the Ames 40- by 80- foot wind tunnel on a wing of A, 4.8; λ, .5; Λ, 35°.

Figure 16. — Continued.

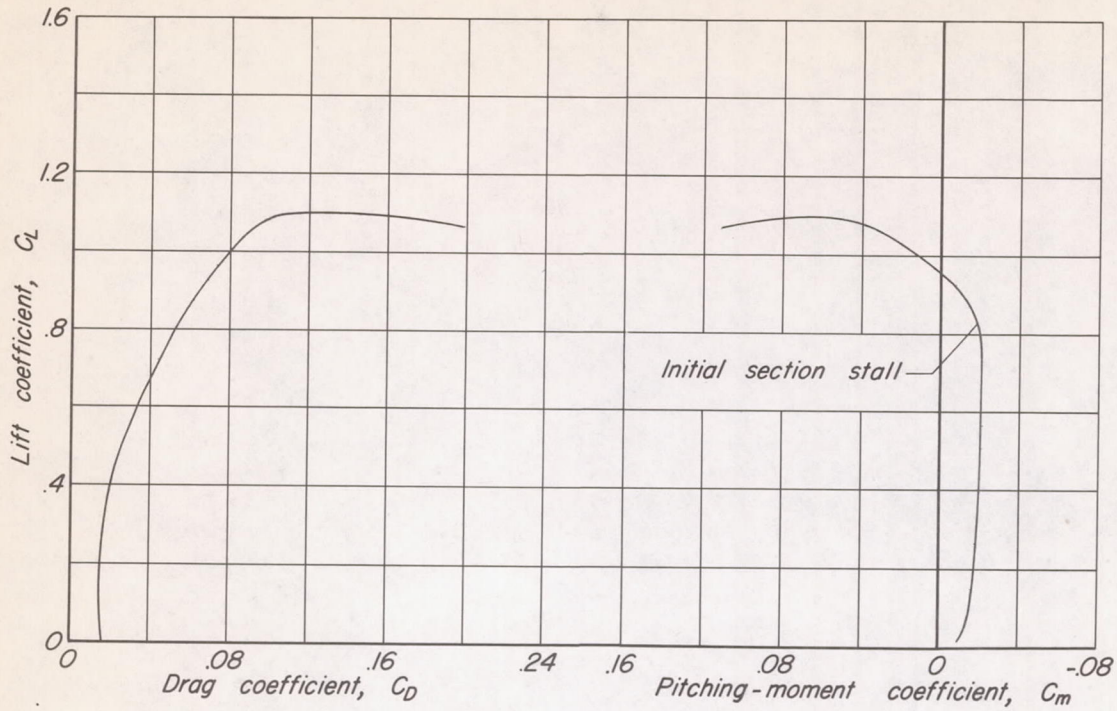

(d) Wing of reference 8. A, 6; λ, .5; Λ, 45°.

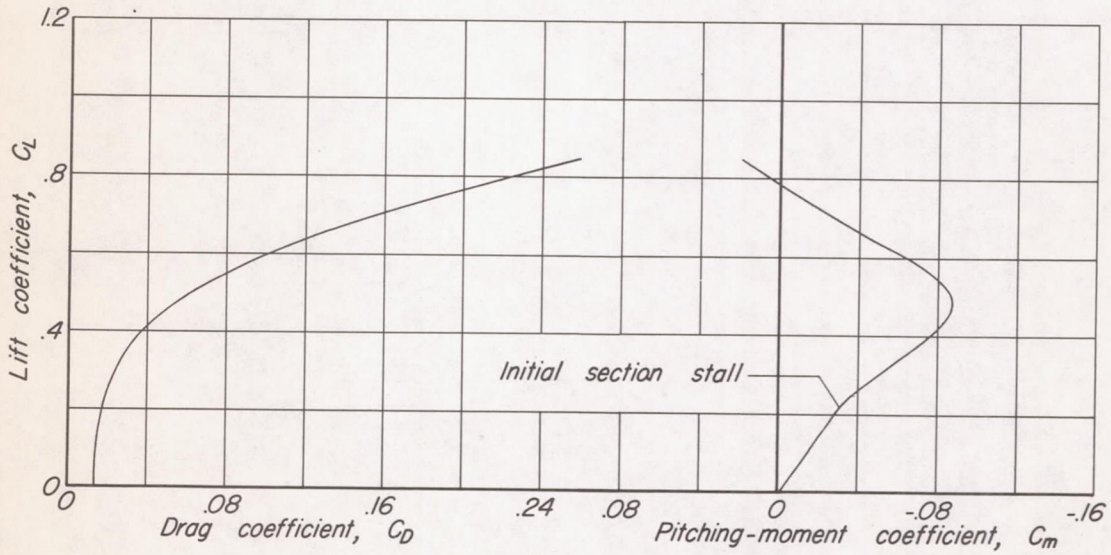

(e) Data from the Ames 40- by 80- foot wind tunnel on a wing of A, 3.5; λ, .25; Λ, 60°.

Figure 16. — Concluded.